1100 V AlGaN/GaN MOSHEMTs With Integrated Tri-Anode Freewheeling Diodes

Taifang Wang, Jun Ma, and Elison Matioli, *Member, IEEE*

***Abstract*— In this letter, we present high-performance reverse-conduction GaN-on-Si metal–oxide–semiconductor high-electron-mobility transistors (RC-MOSHEMTs) with integrated tri-anode freewheeling diodes. Tri-anode Schottky barrier diode presenting small turn-ON voltage (V_{ON}), ultra-low reverse leakage current, and high breakdown voltage (V_{BR}) was incorporated at portions of the drift region of AlGaN/GaN MOSHEMTs as freewheeling diodes. The tri-anode RC-MOSHEMTs exhibited outstanding reverse-conduction performance with a small V_{ON} of 0.55 V, along with a high V_{BR} of 1150 V, state-of-the-art low ON-resistance (R_{ON}) of 8.83 Ω · mm, and high-power figure-of-merit (FOM = $V_{BR}{}^2/R_{ON,SP}$) of 1.32 GW/cm^2. These results reveal the potential of the tri-gate/tri-anode technology for future integrated power electronic devices.**

***Index Terms*— GaN, HEMT, reverse conduction, freewheeling diode, Schottky diode, tri-gate, tri-anode, breakdown, leakage current.**

I. Introduction

GaN-on-Si HEMTs are ideal candidates for the next generation of power electronic devices. Low R_{ON} and high V_{BR} can be achieved due to the exceptional properties of GaN, such as large band-gap, and two-dimensional electron gas (2DEG) with high electron mobility and carrier density. Considering its application for power conversion, especially in topologies in which transistors are connected to inductive elements, a reverse conduction path for the current is required to release the stored inductor energy at switching events [1]. In traditional Si- and SiC-based vertical power devices, built-in body diodes can be designed using the doped layers to offer a freewheeling path when the transistor is switched off [1]–[3]. However, such body diodes cannot be formed in lateral GaN HEMTs, due to their unipolar nature and absence of doped layers. In addition, the reverse current of a HEMT, which is dependent on the gate voltage (V_G), is insufficient to offer freewheeling capability [1]. One way to achieve the freewheeling path is by connecting an anti-parallel diode between the source and drain, which provides a path, independent from V_G, for current to flow under reverse drain bias (V_D) [4]. However, using discrete anti-parallel diodes [5] results in extra device area, larger specific on-resistance ($R_{ON,SP}$), and generates additional parasitic components [6]. A compact solution to this issue is to form a SBD on the backside of the GaN-on-Si substrate, which leverages the small V_{ON} of Si SBDs [7]. Nevertheless, this method requires complex Si deep etching process, and the small V_{BR} of Si SBDs hinders the advantage of GaN transistors. Monolithic integration of anti-parallel planar SBDs between drain and gate of HEMT is another area-efficient approach that offers low reverse conduction loss and does not sacrifice the forward performance [8], [9]. But even so, the major limitation of such method is the large reverse leakage current of planar SBDs, which can be a few orders of magnitude higher than the transistors' OFF-state leakage current (I_{OFF}) [8]–[12]. The high reverse leakage current issue was addressed in [6] with an unconventional double channel heterostructure requiring relatively complex etching processes to demonstrate RC-MOSHEMTs.

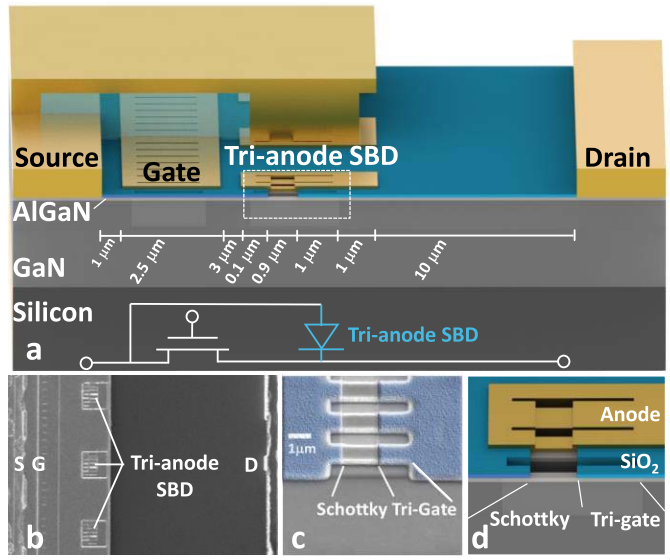

Fig. 1. (a) Schematic and (b) top–view SEM image of the RC-MOSHEMT, (c) zoomed-in SEM image after Schottky contact opening and (d) schematic of tri-anode region.

Alternatively, we have recently shown the outstanding potential of tri-anode SBDs [13] with small V_{ON}, high V_{BR} and ultra-low leakage current for high-performance and high-voltage GaN power SBDs [14], [15] and reverse-blocking

Manuscript received May 19, 2018; accepted May 22, 2018. Date of publication May 30, 2018; date of current version June 26, 2018. This work was supported in part by the Swiss National Science Foundation under Assistant Professor (AP) Energy Grant PYAPP2_166901 and in part by the European Research Council under the European Union's H2020 Program/ERC Grant Agreement 679425. The review of this letter was arranged by Editor G. H. Jessen. *(Corresponding authors: Taifang Wang; Elison Matioli.)*

The authors are with the Power and Wide-band-gap Electronics Research Laboratory (POWERlab), École Polytechnique Fédérale de Lausanne, CH-1015 Lausanne, Switzerland (e-mail: taifang.wang@epfl.ch; elison.matioli@epfl.ch).

Color versions of one or more of the figures in this letter are available online at http://ieeexplore.ieee.org.

Digital Object Identifier 10.1109/LED.2018.2842031

This article has been accepted for publication in a future issue of this journal, but has not been fully edited. Content may change prior to final publication. Citation information: DOI 10.1109/LED.2018.2793669, IEEE Electron Device Letters

transistors [16]. In this work, we demonstrate RC-MOSHEMT with integrated tri-anode SBDs as freewheeling diodes using a relatively simple process. The tri-anode RC-MOSHEMTs presented excellent reverse-conduction capability (V_{ON} = 0.55 V), strong voltage-blocking ability (I_{OFF} = 25 nA/mm at 200 V and V_{BR} = 1150 V at 1 μA/mm with floating substrate), and a record small forward-conduction R_{ON} (8.83 $\Omega \cdot$ mm).

II. Device Structure and Fabrication

Figures 1(a) and (b) show the schematic and top-view scanning electron microscopy (SEM) image of the tri-anode RC-MOSHEMT. The epitaxy in this work consisted of 5 μm of buffer, 0.3 μm of un-doped GaN channel, 23.9 nm of AlGaN barrier, and 1.8 nm of GaN cap layers. The device fabrication started with e-beam lithography to define the fins in the tri-gate and tri-anode regions. Device isolation was done by inductively coupled plasma (ICP) mesa etching, with a depth of ~180 nm. The fin width in the tri-gate and tri-anode regions were 200 nm and 620 nm, along with a spacing of 200 nm and 110 nm, respectively, which were designed based on our previous studies to balance of ON- and OFF-state performances of the device [13], [17]. Source and drain ohmic contacts were formed by alloying Ti/Al/Ti/Ni/Au. A 17 nm thick SiO_2 was deposited by atomic layer deposition (ALD) as the gate dielectric, which was then selectively removed by CHF_3/SF_6-based ICP in the Schottky contact region of tri-anode SBDs (Fig. 1(c)). The anode and gate were formed by Ni/Au (Fig. 1(d)), followed by the deposition of 50 nm-thick ALD SiO_2 interlayer dielectric (ILD) and the second Ni/Au metal layer (M2) as the source-to-anode connection.

The tri-anode RC-MOSHEMTs consisted of a tri-gate MOSHEMT and hybrid tri-anode SBDs integrated in its access region between the gate and drain. To equilibrate the forward and reverse current, 33% of the channel width was occupied by the SBDs, which defines a filling factor (FF) as the width of SBDs divided by the width of device footprint, which will be discussed later. All measurement results in this work were normalized by the width of the device footprint, which was 60 μm. Most of results used the dimensions shown in Fig. 1 (a), unless otherwise specified.

III. Results and Discussion

As shown in Fig. 2(a), the integrated tri-anode SBDs enhanced significantly the reverse conduction performance of the transistors (Fig. 2(a)). The tri-anode RC-MOSHEMTs presented a V_{ON} as small as 0.55 V (at I_D = 1 mA/mm), along with a small reverse forward voltage (V_F) of 1.5 V (at I_D = 50 mA/mm) at $V_G = -7$ V. In contrast, the V_{ON} and V_F of the reference MOSHEMT consisting of a tri-gate structure with L_{GD} of 15 μm were 2.70 V and 4.15 V at the same V_G, respectively. The small V_{ON} is due to the direct contact of the metal to the 2DEG in the tri-anode SBDs [13], [18]. In forward-conduction mode, the tri-anode RC-MOSHEMTs presented a small R_{ON} of 8.83 Ω·mm, which is comparable to the reference device (7.69 Ω·mm), and yields the smallest R_{ON} among reverse-conduction GaN transistors reported in literature. The RC-MOSHEMTs also presented

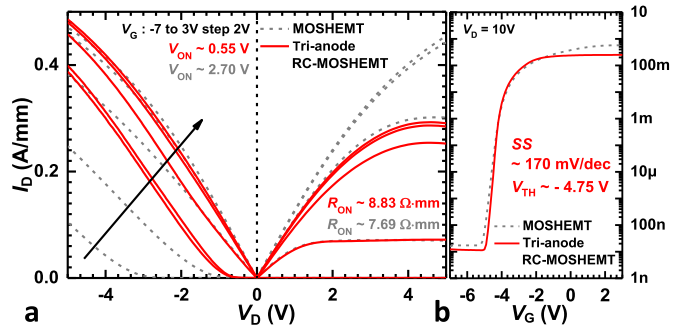

Fig. 2. (a) Output and (b) transfer characteristics of the tri-anode RC-MOSHEMT and MOSHEMT, normalized by the width of the device footprint.

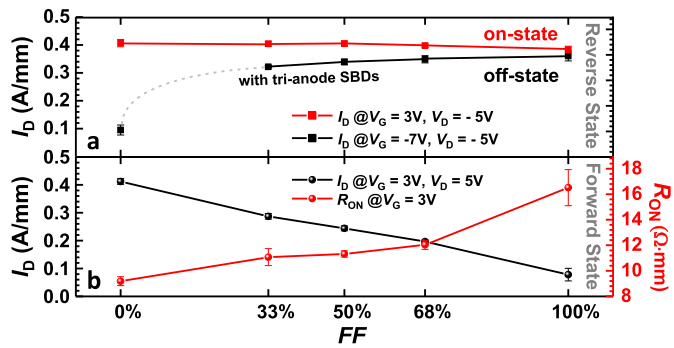

Fig. 3. (a) Reverse and (b) forward characteristics of the tri-anode RC-MOSHEMT with L_{GD} of 21 μm versus different filling factor (FF).

small I_{OFF} and high ON/OFF ratio, which were identical to the reference devices (Fig. 2(b)), due to the small reverse leakage current of the hybrid tri-anode SBDs [13], [15], [19].

The small R_{ON} achieved in the tri-anode RC-MOSHEMTs is mainly attributed to the optimized FF, as it determines the percentage of the channel width used for forward and reverse current conduction. Figure 3(a) plots the I_D in reverse-conduction mode of the tri-anode RC-MOSHEMTs (L_{GD} = 21 μm, at $V_D = -5$ V) as a function of their FFs. When V_G is higher than V_{TH}, the reverse I_D is independent of the FF as the transistor is in ON-state. When V_G is below V_{TH}, FF = 33% is already large enough to nearly saturate the reverse I_D. This indicates that a small FF value is already enough for tri-anode SBDs to extract most of electrons injected from drain side. In forward-conduction mode, the I_D decreases while the R_{ON} increases with increasing FF (Fig. 3(b)), which is caused by the smaller effective channel width and higher spreading resistance. Based on these results, a FF of 33% was selected, which provided high freewheeling current with small degradation in the forward performance, resulting in a record small R_{ON}, which is highly desirable for efficient power conversion.

The tri-anode RC-MOSHEMT presented good reverse-conduction performance at high temperature. From 25 °C to 150 °C, the V_{ON} increased to 0.63 V, and the reverse current reduced to 213 mA/mm (at $V_D = -5$ V) (Fig. 4(a)). In forward bias, the R_{ON} was 20.69 $\Omega \cdot$ mm at 150 °C, which is comparable to other integrated devices [6], [16], revealing the great potential for high temperature applications (Fig. 4(b)).

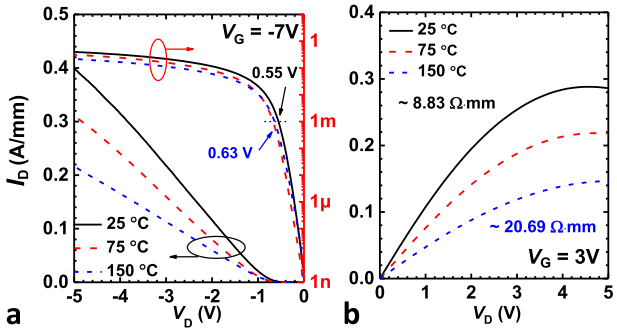

Fig. 4. Temperature dependent (a) reverse and (b) forward output characteristics of the tri-anode RC-MOSHEMT at 25 °C, 75 °C and 150 °C.

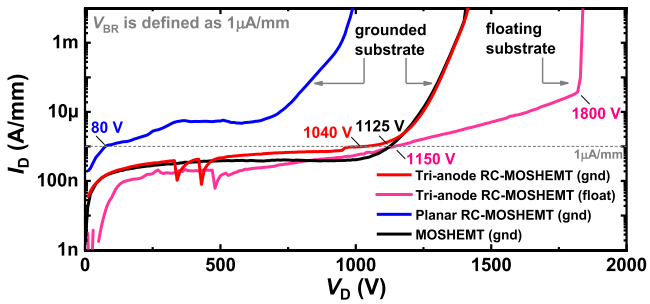

Fig. 5. Breakdown characteristics of the tri-anode RC-MOSHEMT with grounded substrate (gnd) and floating substrate (float), along with the reference planar RC-MOSHEMT (gnd) and MOSHEMT (gnd).

Figure 5 shows the breakdown characteristics of the tri-anode RC-MOSHEMT and reference devices. The V_{BR} of tri-anode RC-MOSHEMT was 1040 V, which is close to that of the reference MOSHEMT (tri-gate MOSHEMT with L_{GD} = 15 μm) and significantly improved as compared to the planar RC-MOSHEMT (planar MOSHEMT with planar SBDs, and L_{GD} of 20 μm). Such enhancement in V_{BR} is attributed to the better leakage control capability of integrated tri-anode SBDs [15], [19]–[21]. In addition, a very small I_{OFF} of 0.6 μA/mm at 650 V was observed for the tri-anode RC-MOSHEMTs, which is due to the reduced voltage drop at the Schottky junction in the hybrid tri-anode SBDs [15], [19]. With floating substrate, the V_{BR} of the RC-MOSHEMTs was as high as 1150 V at 1 μA/mm, and the hard breakdown (HBD) did not occur until 1800 V due to better-distributed electric field of tri-gate MOSHEMTs [14], [15].

The RC-MOSHEMTs with integrated tri-anode SBDs were compared with other literature results of reverse-conduction GaN transistors in Tab. 1, presenting small R_{ON}, V_{ON}, and I_{OFF}, along with the highest V_{BR} of 1040 V. We further benchmarked the tri-anode RC-MOSHEMTs against state-of-the-art discrete lateral GaN-on-Si (MOS)HEMTs, SBDs and other reported RC-MOSHEMTs in Fig. 6, showing V_{BR} and $R_{ON,SP}$ comparable to discrete MOSHEMTs and SBDs, and outperforming other reported reverse-conduction transistors. These results reveal the significant potential of the tri-gate/tri-anode technology for highly integrated GaN power devices.

TABLE I
COMPARISON OF THE TRI-ANODE RC-MOSHEMT IN THIS WORK WITH OTHER REVERSE-CONDUCTION TRANSISTORS IN THE LITERATURE

	This work	[6]	[9]	[7]	[11]
Type	D-mode	E-mode	D-Mode	D-mode	E-mode
R_{ON} (Ω·mm)	8.83	12.1	10.95	--	26
V_{ON} (@1mA/mm)	0.55 V	0.6 V	--	--	0.8 V
ON/OFF Ratio	8	7	5	10	--
I_{OFF} (@200V)	25 nA/mm	18 nA/mm	>1 μA/mm	--	--
V_{BR} (@1μA/mm)	1040 V	698 V	<10 V	<30 V	<100 V
V_{BR} (hard breakdown)	1800 V	--	800 V	--	966 V

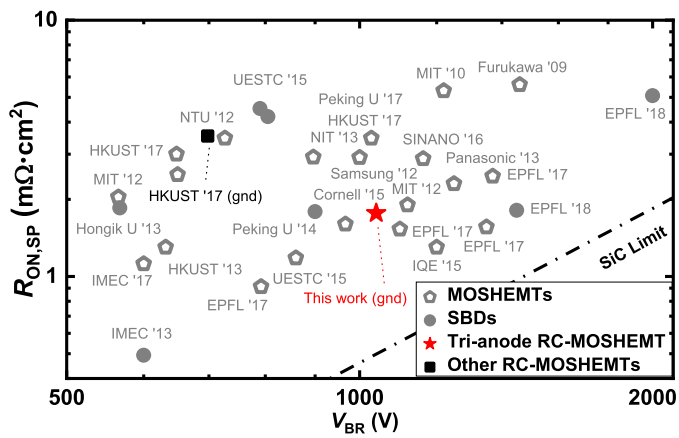

Fig. 6. $R_{ON,SP}$ versus V_{BR} benchmark of the tri-anode RC-MOSHEMT with against GaN-on-Si power MOSHEMTs and lateral SBDs. The V_{BR} was defined at 1 μA/mm and a 15 μm transfer length of source/drain was considered for the calculation of $R_{ON,SP}$. Only V_{BR} larger than 500 V have been considered in this benchmark.

IV. CONCLUSION

In this work we presented reverse-conduction GaN-on-Si MOSHEMTs with state-of-the-art performance, by integrating tri-anode freewheeling SBDs. The devices exhibited excellent reverse performance, along with a record small R_{ON}, which can be promising for the next-generation of efficient power converters.

REFERENCES

[1] A. Lidow, J. Strydom, M. de Rooij, and Y. Ma, *GaN Transistors for Efficient Power Conversion*. El Segundo, CA, USA: Efficient Power Conversion Corporation, 2012, doi: 10.1002/9781118844779.

[2] K. Kawahara, S. Hino, K. Sadamatsu, Y. Nakao, Y. Yamashiro, Y. Yamamoto, T. Iwamatsu, S. Nakata, S. Tomohisa, and S. Yamakawa, "6.5 kV Schottky-barrier-diode-embedded SiC-MOSFET for compact full-unipolar module," in *Proc. 29th Int. Symp. Power Semiconductor Devices IC's (ISPSD)*, Sapporo, Japan, May/Jun. 2017, pp. 41–44, doi: 10.23919/ISPSD.2017.7988888.

[3] H. Ruthing, F. Hille, F.-J. Niedernostheide, H.-J. Schulze, and B. Brunner, "600 V reverse conducting (RC-)IGBT for drives applications in ultra-thin wafer technology," in *Proc. 19th Int. Symp. Power Semiconductor Devices*, Jeju Island, South Korea, May 2007, pp. 89–92, doi: 10.1109/ISPSD.2007.4294939.

[4] D. K. Saini, A. Ayachit, M. K. Kazimierczuk, and T. Suetsugu, "Buck DC-AC converter using gallium-nitride FETs for amplitude-modulated class-E RF power amplifiers," in *Proc. 41st Annu. Conf. IEEE Ind. Electron. Soc. (IECON)*, Yokohama, Japan, Nov. 2015, pp. 003579–003584, doi: 10.1109/IECON.2015.7392656.

[5] T. Kachi, M. Kanechika, and T. Uesugi, "Automotive applications of GaN power devices," in *Proc. IEEE Compound Semiconductor Integr. Circuit Symp. (CSICS)*, Waikoloa, HI, USA, Oct. 2011, pp. 1–3, doi: 10.1109/CSICS.2011.6062459.

[6] J. Lei, J. Wei, G. Tang, Q. Qian, M. Hua, Z. Zhang, Z. Zheng, and K. J. Chen, "An interdigitated GaN MIS-HEMT/SBD normally-off power switching device with low ON-resistance and low reverse conduction loss," in *IEDM Tech. Dig.*, San Francisco, CA, USA, Dec. 2017, pp. 25.2.1–25.2.4, doi: 10.1109/IEDM.2017.8268456.

[7] T. Morita, S. Ujita, H. Umeda, Y. Kinoshita, S. Tamura, Y. Anda, T. Ueda, and T. Tanaka, "GaN gate injection transistor with integrated Si Schottky barrier diode for highly efficient DC-DC converters," in *IEDM Tech. Dig.*, San Francisco, CA, USA, Dec. 2012, pp. 7.2.1–7.2.4, doi: 10.1109/IEDM.2012.6478996.

[8] R. Reiner, P. Waltereit, B. Weiss, M. Wespel, M. Mikulla, R. Quay, and O. Ambacher, "Monolithic GaN-on-Si half-bridge circuit with integrated freewheeling diodes," in *Proc. Eur. Int. Exhib. Conf. Power Electron., Intell. Motion, Renew. Energy Energy Manage. (PCIM)*, Nuremberg, Germany, May 2016, pp. 1–7.

[9] R. Reiner, P. Waltereit, B. Weiss, M. Wespel, R. Quay, M. Schlechtweg, M. Mikulla, and O. Ambacher, "Integrated reverse-diodes for GaN-HEMT structures," in *Proc. IEEE 27th Int. Symp. Power Semiconductor Devices IC's (ISPSD)*, Hong Kong, May 2015, pp. 45–48, doi: 10.1109/ISPSD.2015.7123385.

[10] B.-R. Park, J.-G. Lee, and H.-Y. Cha, "Normally-off AlGaN/GaN-on-Si power switching device with embedded Schottky barrier diode," *Appl. Phys. Express*, vol. 6, pp. 031001-1–031001-3, Feb. 2013, doi: 10.7567/APEX.6.031001.

[11] B.-R. Park, J.-Y. Lee, J.-G. Lee, D.-M. Lee, M.-K. Kim, and H.-Y. Cha, "Schottky barrier diode embedded AlGaN/GaN switching transistor," *Semicond. Sci. Technol.*, vol. 28, p. 125003, Oct. 2013, doi: 10.1088/0268-1242/28/12/125003.

[12] R. Reiner, P. Waltereit, B. Weiss, R. Quay, and O. Ambacher, "Investigation of GaN-HEMTs in reverse conduction," in *Proc. Eur. Int. Exhib. Conf. Power Electron., Intell. Motion, Renew. Energy Energy Manage.*, Nuremberg, Germany, May 2017, pp. 1–8.

[13] E. Matioli, B. Lu, and T. Palacios, "Ultralow leakage current AlGaN/GaN Schottky diodes with 3-D anode structure," *IEEE Trans. Electron Devices*, vol. 60, no. 10, pp. 3365–3370, Oct. 2013, doi: 10.1109/TED.2013.2279120.

[14] J. Ma and E. Matioli, "High-voltage and low-leakage AlGaN/GaN tri-anode Schottky diodes with integrated tri-gate transistors," *IEEE Electron Device Lett.*, vol. 38, no. 1, pp. 83–86, Jan. 2017, doi: 10.1109/LED.2016.2632044.

[15] J. Ma and E. Matioli, "2 kV slanted tri-gate GaN-on-Si Schottky barrier diodes with ultra-low leakage current," *Appl. Phys. Lett.*, vol. 112, pp. 052101-1–052101-4, Jan. 2018, doi: 10.1063/1.5012866.

[16] J. Ma, M. Zhu, and E. Matioli, "900 V reverse-blocking GaN-on-Si MOSHEMTs With a hybrid tri-anode Schottky drain," *IEEE Electron Device Lett.*, vol. 38, no. 12, pp. 1704–1707, Dec. 2017, doi: 10.1109/LED.2017.2761911.

[17] J. Ma and E. Matioli, "High performance tri-gate GaN power MOSHEMTs on silicon substrate," *IEEE Electron Device Lett.*, vol. 38, no. 3, pp. 367–370, Mar. 2017, doi: 10.1109/LED.2017.2661755.

[18] J. Ma, G. Santoruvo, P. Tandon, and E. Matioli, "Enhanced electrical performance and heat dissipation in AlGaN/GaN Schottky barrier diodes using hybrid tri-anode structure," *IEEE Trans. Electron Devices*, vol. 63, no. 9, pp. 3614–3619, Jul. 2016, doi: 10.1109/TED.2016.2587801.

[19] J. Ma, D. C. Zanuz, and E. Matioli, "Field plate design for low leakage current in lateral GaN power Schottky diodes: Role of the pinch-off voltage," *IEEE Electron Device Lett.*, vol. 38, no. 9, pp. 1298–1301, Sep. 2017, doi: 10.1109/LED.2017.2734644.

[20] J.-Y. Lee, B.-R. Park, H. Kim, J. Kim, and H.-Y. Cha, "AlGaN/GaN MOSHFET power switching transistor with embedded fast recovery diode," *Electron. Mater. Lett*, vol. 10, no. 6, pp. 1115–1120, Nov. 2014, doi: 10.1007/s13391-014-4128-0.

[21] J. Ma and E. Matioli, "Slanted tri-gates for high-voltage GaN power devices," *IEEE Electron Device Lett.*, vol. 38, no. 9, pp. 1305–1308, Sep. 2017, doi: 10.1109/LED.2017.2731799.